Schwyzer, R. (1977) *Ann. N.Y. Acad. Sci. 297*, 3–26.
Schwyzer, R. (1980) *Proc. R. Soc. London, Ser. B 210*, 5–20.
Schwyzer, R. (1985a) in *Natural Products Chemistry 1984* (Zalewski, R. I., & Skolik, J. J., Eds.) pp 591–598, Elsevier, Amsterdam.
Schwyzer, R. (1985b) in *Peptides: Structure and Function* (Deber, C. M., Hruby, V. J., & Kopple, K. D., Eds.) pp 3–12, Pierce Chemical Co., Rockford, IL.
Schwyzer, R. (1986) *Biochemistry 25*, 4281–4286.
Schwyzer, R., Gremlich, H.-U., Gysin, B., Sargent, D. F., & Fringeli, H.-P. (1983) in *Peptides: Structure and Function* (Hruby, V. J., & Rich, D. H., Eds.) pp 657–664, Pierce Chemical Co., Rockford, IL.
Von Heijne, G. (1981) *Eur. J. Biochem. 116*, 419–422.
Von Heijne, G., & Blomberg, C. (1979) *Eur. J. Biochem. 97*, 175–181.

Conformational Transitions in N-Linked Oligosaccharides†

S. W. Homans,*,‡ R. A. Dwek,*,‡ J. Boyd,‡ M. Mahmoudian,§ W. G. Richards,§ and T. W. Rademacher*,‡
Departments of Biochemistry and Physical Chemistry, University of Oxford, Oxford OX1 3QU, Great Britain
Received April 4, 1986; Revised Manuscript Received June 5, 1986

ABSTRACT: An assignment strategy involving ^1H–^1H correlated spectroscopy (COSY), relayed correlation spectroscopy (RECSY), nuclear Overhauser effect spectroscopy (NOESY), and triple quantum filtered correlated spectroscopy (TQCOSY) is described for six related N-linked oligosaccharides. These are of three "types", i.e., complex, bisected complex, and oligomannose. Using spin–spin coupling constant data derived from these assignments, together with semiempirical quantum mechanical energy calculations, we have examined the rotamer distributions at the Manα1–6Manβ– linkage in each structure, and additionally at the Manα1–6Manα– linkage in oligomannose oligosaccharides. We show that while several primary sequence differences are "passive", certain key residues modulate the orientation of the α1–6 arms. These residues may be proximal or distal to the site of the conformational change. There is no direct correlation between these perturbations and the oligosaccharide type. These data are discussed in terms of the proposed recognition function of oligosaccharides in biological systems.

The role of oligosaccharides as modulators of cell–cell recognition has been implicated in a variety of systems (Ivatt, 1984). Oligosaccharides in secreted and cell-surface glycoproteins (Ivatt, 1984; Fukuda & Fukuda, 1984) and cell-surface glycolipids (Feizi, 1981) are known to change during developmental and transformational events. This implies that the precise spatial and temporal disposition of a cell is communicated to the external milieu by oligosaccharide-dependent recognition phenomena. Studies on the conformational properties of oligosaccharides may lead to a better understanding of the molecular basis of these events. In principle, small differences in oligosaccharide primary sequence could lead to new conformational determinants, and two mechanisms can be envisaged whereby this might occur.

In the first mechanism, the addition of a monosaccharide residue generates a new determinant and masks others (or conversely, a deletion results in the loss of a determinant and the reexposure of masked residues). No significant conformational change need occur in the overall structure. This mechanism is known to exist in blood group determinants (Szulman, 1980) and in glycolipid differentiation antigens (Feizi, 1981). The second mechanism involves the addition or deletion of a monosaccharide which may lead to a conformational rearrangement of preexisting determinants either adjoining or distal to the added or deleted residue. This could create a totally new overall conformation which may form a new determinant not involving the added monosaccharide. The nascent ligand generated by the second mechanism would be difficult to predict from the primary sequence.

The determination of the three-dimensional structures of oligosaccharides with related but distinct primary sequence is a first step in studying the above events, thereby leading to a better understanding of the proposed roles of oligosaccharides not only as recognition signals but also as possible structural elements. At present, the only method with which to determine oligosaccharide solution conformations with accuracy is high-resolution NMR.[1] Our early one- and two-dimensional ^1H NMR studies (Homans et al., 1982, 1983a) showed that the biantennary *oligosaccharide* derived from human serotransferrin exists in solution with regions of defined secondary structure. Subsequently, Brisson and Carver have investigated the solution conformations of a variety of *glycopeptides* (Brisson & Carver, 1983a,b) and found that conformational variance was primarily associated with the Manα1–6Manβ1– linkage of the core. More specifically, the rotamer distributions about the C5–C6 bond of the Manβ1–residue were found to depend upon the oligosaccharide "class" (i.e., oligomannose, complex, bisected complex, and hybrid). An important consequence of such structural changes is that the *overall* solution

† This work is a contribution from the Oxford Oligosaccharide Group, which is supported by Monsanto. S.W.H., R.A.D., J.B., W.G.R., and T.W.R. are members of the Oxford Enzyme Group.
‡ Department of Biochemistry.
§ Department of Physical Chemistry.

[1] Abbreviations: NMR, nuclear magnetic resonance; COSY, ^1H–^1H correlated spectroscopy; TQCOSY, triple quantum filtered ^1H–^1H correlated spectroscopy; NOE, nuclear Overhauser effect; NOESY, nuclear Overhauser effect spectroscopy; 1D, one dimensional; 2D, two dimensional; MNDO, modified neglect of diatomic differential overlap; RECSY, multiple-step relayed correlation spectroscopy.

0006-2960/86/0425-6342$01.50/0

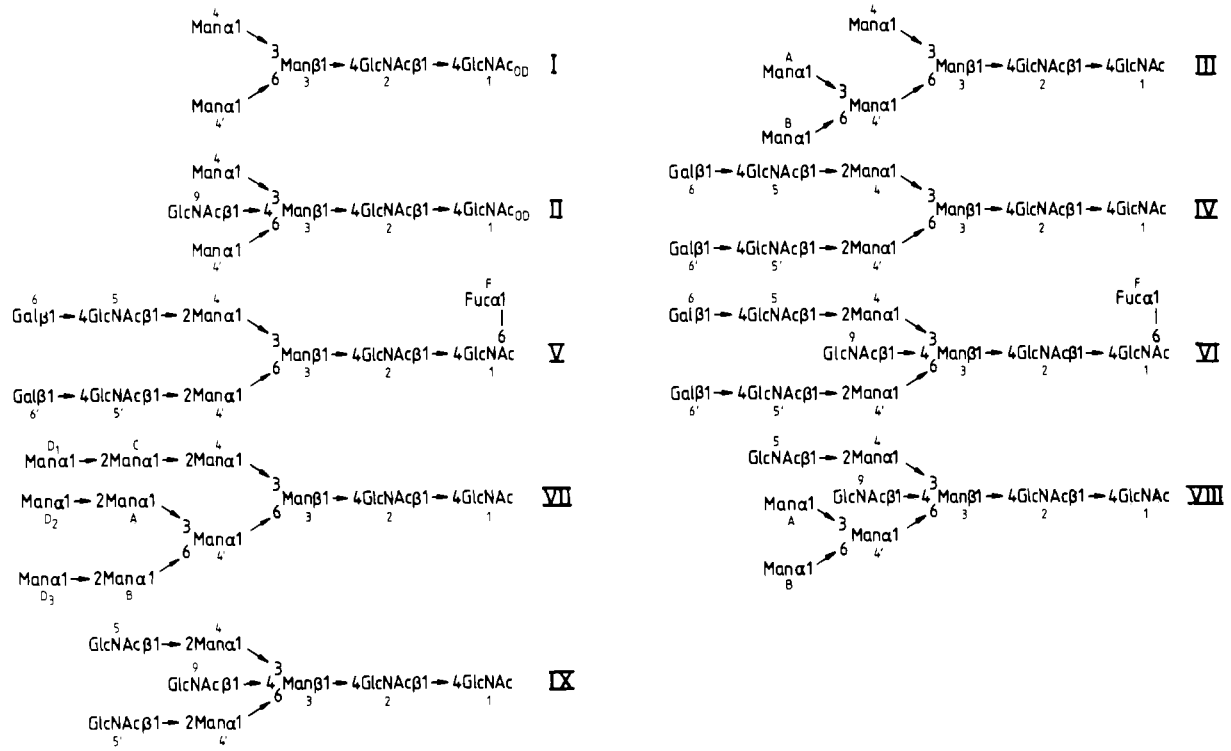

FIGURE 1: Structures of oligosaccharides described in the present study. Experimental data are presented for compounds I–IV, VI, and VII. In addition, reference is made in the text to structures V, VIII, and IX, which have been investigated previously by Brisson and Carver (1983b) (structures V and VIII) and by Strecker et al. (1977) (structure IX). The subscript OD indicates oligosaccharides reduced with sodium borodeuteride.

conformation of the oligosaccharide is altered. This is therefore relevant to the mechanisms proposed above.

In this study we have undertaken a detailed analysis of the factors that influence the distribution of rotamers at α1–6 linkages, in six related N-linked oligosaccharides (structures I–IV, VI, and VII in Figure 1). In addition, we incorporate the work of others on structures V, VIII, and IX into our discussion as described later. The conformational analysis has been achieved by measurement of the rotamer-sensitive mutual spin–spin couplings (J's) within the H5, H6, and H6′ spin subsystem of Man-3 in each oligosaccharide, and for the corresponding protons of Man-4′ at the additional α1–6 linkage in high-mannose structures III and VII. In conventional 2D spectra, these parameters are difficult to extract due to overlap of cross-peaks between resonances from the same residue. As an alternative, one-dimensional NOE difference spectroscopy has been used to determine the multiplicity of the relevant multiplets (Brisson & Carver, 1983b), but in our experience the J's are difficult to measure from the difference spectrum. Furthermore, the correct assignments must still be known with complete confidence. Indeed, several groups (Brisson & Carver, 1983b; Paulsen et al., 1984; Bock et al., 1982) have previously investigated the solution conformations about α1–6 linkages in oligosaccharides. There are discrepancies between the proposed assignments for the relevant H6 protons and their respective J values. Here, we present an alternative assignment strategy for each oligosaccharide "type", using ^{1}H–^{1}H correlated spectroscopy (COSY), multiple-step relayed correlation spectroscopy (RECSY), nuclear Overhauser effect spectroscopy (NOESY), and COSY simplified by filtration through triple quantum coherence (TQCOSY). This allows an essentially complete set of resonance asssignments and J's to be obtained, which greatly reduces any assignment ambiguity. The measured J values, together with semiempirical quantum mechanical (MNDO) energy calculations to predict the allowed energy minima about the C5–C6 bond in model monosaccharides, allow for a straightforward analysis of the conformational variance between the oligosaccharides investigated here.

Materials and Methods

The isolation of compound I from hen ovomucoid by large-scale hydrazinolysis has been described previously (Homans et al., 1984). Compound II (8.2 glucose units) was isolated on a Bio-Gel P-4 (−400 mesh) column (200 cm × 1.5 cm) after the ovomucoid oligosaccharide structures eluting at ~10.5 glucose units were digested with *Streptococcus pneumoniae* β-*N*-acetylhexosaminidase. Compounds III and VII were released from bovine pancreatic ribonuclease (Liang et al., 1980) and soybean agglutinin (Dorland et al., 1981), respectively, by large-scale hydrazinolysis, followed by purification on Bio-Gel P-4 (−400 mesh). Compound III eluted at 8.4 glucose units, and compound VII eluted at 12.3 glucose units. Compound IV was prepared by desialylation using *Arthrobacter ureafaciens* neuraminidase of the disialylated oligosaccharide obtained from human serotransferrin as described previously (Homans et al., 1983a). Compound VI was released from sheep immunoglobulin G by large-scale hydrazinolysis, followed by purification on a column (20 cm × 0.5 cm) of concanavalin A–Sepharose. The unbound fraction was applied to a column of Bio-Gel P-4 (−400 mesh), and compound VI was isolated as the fraction eluting at 14.5 glucose units. Samples were prepared in deuterium oxide for NMR studies as described previously (Homans et al., 1984).

NMR Spectroscopy. Two-dimensional ^{1}H–^{1}H correlated (COSY) spectroscopy and multiple-step relayed correlation spectroscopy (RECSY) were performed at 500 MHz as described previously (Homans et al., 1983b, 1984). In total, 1024 t_1 increments of 32 scans each were recorded with a variable sweep width and 1024 real data points in t_2. The time domain data matrix was "zero-filled" once in each dimension to yield a final resolution of 2048 × 2048 real data points. Triple

quantum filtered COSY spectra were obtained according to Piantini et al. (1982), using similar conditions to those used in COSY experiments, but with 512 t_1 increments of 48 scans each. The theoretical details of triple-quantum COSY are described in the Appendix. Two-dimensional ^1H–^1H phase-sensitive nuclear Overhauser effect (NOESY) experiments were performed according to Müller and Ernst (1980) and States et al. (1982), using identical conditions to those in COSY experiments, although only 512 t_1 increments were collected.

Energy Calculations. Stable rotamers of the hydroxymethyl groups of the model monosaccharides β-D-glucose and β-D-mannose were determined by using both MNDO and for comparison molecular mechanics (MM2) procedures.

Ring carbon atoms in these monosaccharides are designated clockwise C_1 to C_5, with C_1 being the anomeric carbon. The ring oxygen is designated O_5. The remaining hydrogen and oxygen atoms are labeled according to their parent carbon atoms, with hydroxyl protons designated H′. The dihedral angle ω is defined as O6C6C5H5, with positive values of ω corresponding to anticlockwise rotations of O6C6, while looking down the C6C5 bond.

Geometries of β-D-glucose and β-D-mannose were optimized by using the MOPAC program (Stewart, 1984), starting with initial geometries constructed by using the crystal structure of β-D-glucose (Chu & Jeffrey, 1968). These initial geometries were used as input to a new variation of the semiempirical all-valence electron molecular orbital method, MNDO (Dewar & Thiel, 1977). This variation is a new parametrization of the MNDO method following recent suggestions of Dewar et al. (1985) to predict accurately the formation of hydrogen bonding.

In addition to finding the minimum energy conformer of β-D-glucose resulting from the MOPAC geometry optimization, a more detailed conformational energy calculation was made to determine other possible conformers. The hydroxymethyl group of β-D-glucose was rotated in 15° steps and the total energy of the molecule calculated by using the quantum chemical method or, for comparison, the molecular mechanics method MM2 (Allinger & Yuh, 1981).

Alternatively, to take into account the possibility that H′4 may hydrogen bond with the hydroxymethyl oxygen (O6), the dihedral angle H′6O6C6C5 was kept at 180° and the bond lengths and angles of OH4 were optimized during rotation of the hydroxymethyl group. The energy calculation was carried out by using the quantum chemical method as described above. Finally, for the possibility that both H′6 and H′4 may form hydrogen bonds with the solvent, the dihedral angles of both H′6O6C6C5 and H′4O4C4C5 were fixed at 180°, and the energy of the molecule for each 15° step of the rotation of the hydroxymethyl group was calculated as above. The range of conformations that encompassed 99%, 95%, and 70% of the molecules at 37 °C was calculated by using a statistical mechanical procedure on the computed potential surface (Richards & Ganellin, 1974). A similar series of calculations was carried out for β-D-mannose.

RESULTS

Resonance Assignments and J's. The oligosaccharides under investigation are representative of three types: complex (structures I and IV in Figure 1), oligomannose (structures III and VII), and bisected complex (structures II and VI). the assignment strategy in each structure is similar, involving the determination of an essentially complete, self-consistent set of assignments to minimize ambiguity. However, the assignment methods employed vary between the types, and these are therefore discussed in turn.

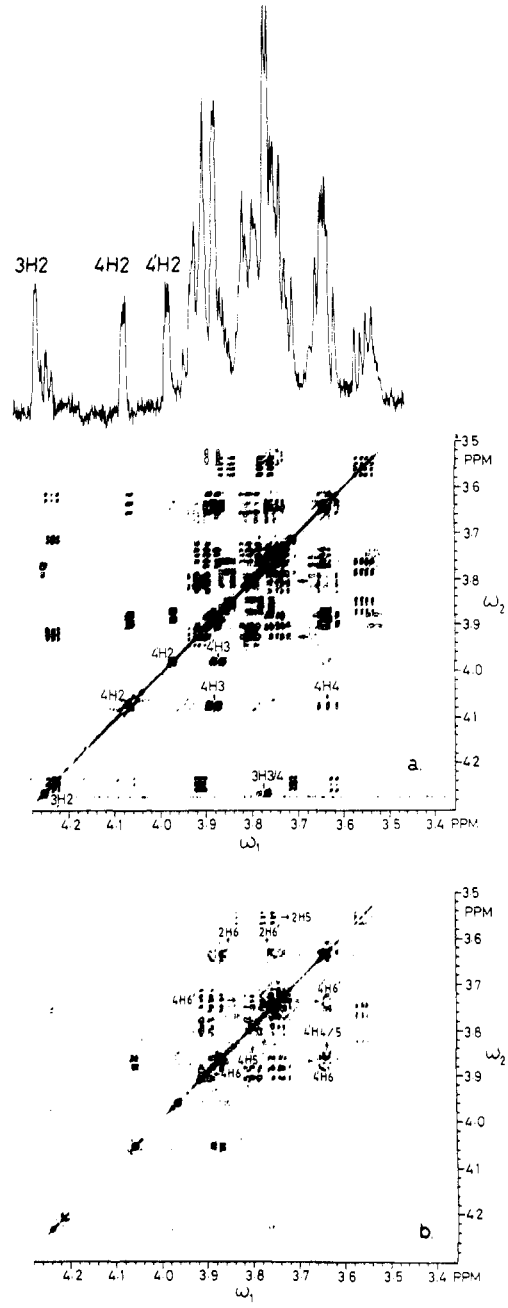

FIGURE 2: (a) COSY spectrum (region 3.4–4.5 ppm) of oligosaccharide I. Resonance assignments can be made for several protons in the normal manner as illustrated for mannose residues 3, 4, and 4′ (see Figure 1 for nomenclature). However, cross-peak overlap does not allow the H5 and H6 proton resonance assignments to be obtained unambiguously. (b) Triple quantum COSY spectrum (region 3.4–4.5 ppm) of oligosaccharide I. The number of cross-peaks is reduced in comparison with spectrum a, and these correlate exclusively the H5 and H6 protons as shown. An exception is seen in the cross-peak correlating Man-4 H2 with Man-4 H3 ($\omega_1 \approx 3.87$ ppm, $\omega_2 \approx 4.05$ ppm). This cross-peak is not purged in the TQCOSY spectrum due to the resolved coupling between Man-4 H2 and Man-4 H4 (see spectrum a). In both spectrum a and spectrum b, the *N*-acetyl methyl protons of GlcNAc-1 and GlcNAc-2 have been aliased into the spectrum ($\omega_1 \approx \omega_2 = -4.08$ ppm) to improve digital resolution.

Resonance Assignments and J's in Complex Type Oligosaccharides. The determination of proton resonance assignments in complex type structures is exemplified with reference to structure I. Preliminary resonance assignments are made in I by using ^1H–^1H COSY (Figure 2). While several assignments can be made in the normal manner from the COSY

spectrum (see Figure 2a), a large number are still unavailable due to cross-peak overlap. We have previously demonstrated the use of multistep relayed correlation spectroscopy (RECSY) to make further assignments in this compound (Homans et al., 1984). However, although the H5 proton assignments were available for the majority of residues, unambiguous assignments could not be made for any of the H6 protons with complete confidence. In the present study we employ triple quantum filtered COSY (TQCOSY) for this purpose (Piantini et al., 1982). The triple quantum filter purges the COSY spectrum of all cross-peaks except those corresponding to correlations between H5, H6, and H6′ protons (see Appendix). A TQCOSY spectrum of I is shown in Figure 2b. The number of cross-peaks is clearly greatly reduced in comparison with conventional COSY. Taking into account the H5 proton resonance assignments obtained from RECSY, the assignment of the H6 protons follows directly by inspection of Figure 2b, as shown, with the exception of the H6 protons of Man-3 (see Figure 1 for nomenclature). These are now obtained by a process of elimination from the conventional COSY spectrum (Figure 2a). The low intensity of the relevant cross-peaks is explained by the strong coupling of the H3 and H4 resonances of Man-3 (Homans et al., 1984), which thus broadens the H5 proton resonance by the nature of its multiplicity. Having identified the relevant cross-peaks, couplings between H5, H6, and H6′ for Man-3 could be measured directly from the COSY spectrum. However, the relative resonance positions of the chemically equivalent H6 protons, and thus the values of J_{56} and $J_{56'}$, could not be formally determined. Although this information has been obtained unambiguously in monosaccharide derivatives (Gagnaire et al., 1973), extrapolation of these data to oligosaccharides is not valid. We find later that only one of the possible pairs of assignments is consistent with the results of semiempirical quantum mechanical energy calculations.

By use of entirely analogous methods, proton resonance assignments and J's for the H5, H6, and H6′ protons of IV were determined (data not shown).

Resonance Assignments and J's in Oligomannose Type Oligosaccharides. As in structures I and IV, initial assignments were obtained in VII by using COSY (Figure 3). Due to the large degree of symmetry and repeating structure, a large number of mannosyl resonance cross-peaks were found to be degenerate. Thus, for VII, the use of RECSY was found to be mandatory. The relevant cross sections along ω_1 from the RECSY spectrum are shown in Figure 4. The correlations of H1 for each mannose residue with H2, H3, H4, and H5 are used to resolve assignment ambiguity from COSY. Cross sections for Man-3 and Man-4′ are not shown, since transfer was incomplete due to unsuitable coupling topography. In the absence of assignments for Man-3 H5 and Man-4′ H5, the corresponding H6 protons could thus not be obtained unambituously from the TQCOSY spectrum (data not shown). A complete assignment strategy was thus not possible by using coherence transfer methods alone. However, it is well-known that intraresidue and interresidue nuclear Overhauser effects (NOE's) may be used as an assignment aid. Although these are not universally applicable due to the correlation time dependence of the NOE, the use of pure absorption mode two-dimensional NOE (NOESY) experiments was found to be useful in VII. In the NOESY spectrum of VII (Figure 3), Man-3 H5 was assigned from an intraresidue NOE to Man-3 H1. By use of the data obtained from COSY and RECSY of VII, the remainder of the cross-peaks in the NOESY spectrum could be assigned. The H6 proton resonance as-

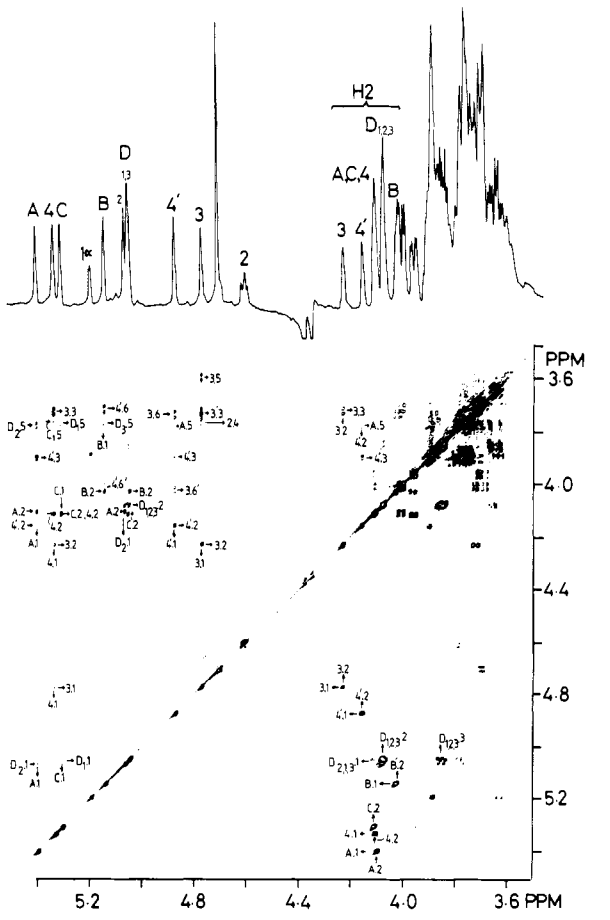

FIGURE 3: COSY spectrum (lower right) and NOESY spectrum (upper left) of oligosaccharide VII. Only a small fraction of resonance assignments (H1's, H2's, and some H3's) are available from the COSY spectrum due to severe resonance overlap. These are obtained in the normal manner as shown. The assignments shown for the cross-peaks in the NOESY spectrum were obtained from COSY and RECSY, and by consideration of intraresidue and interresidue NOE's (see Figure 4 and text).

signments of Man-3 and of Man-4′ were obtained from interresidue NOE's from Man-4′ H1 and Man-B H1, respectively, the relevant cross-peaks being identified by a process of elimination. Importantly, the correlation of the H6 protons with each other for both Man-3 and Man-4′ was then obvious in the COSY (Figure 3) spectrum, thus leading to self-consistent assignments. The corresponding J values were most easily extracted from the NOESY spectrum.

The relevant assignments and J's in III were obtained by analogous methods to those described above for VII (data not shown).

Resonance Assignments and J's in Bisected Complex Type Oligosaccharides. The majority of proton resonance assignments in VI were available from the conventional COSY experiment (Figure 5a), since the perturbing influence of the "bisecting" GlcNAc was found to cause greater chemical shift dispersion than in complex or high-mannose type oligosaccharides. Thus, the H5 proton resonance of Man-3 could be obtained directly from the COSY spectrum (see Figure 5a). The H6 proton resonance assignments were then obtained as before by using TQCOSY (Figure 5b). It was found that the H5 and H6 protons formed an approximate A_2X system, with the H6 protons resonating in almost identical positions. It was thus not possible to measure the respective J values directly. However, with the resonance assignments obtained from TQCOSY, the multiplicity of Man-3 H5 could be directly obtained in a cross section from COSY (Figure 5a), and the

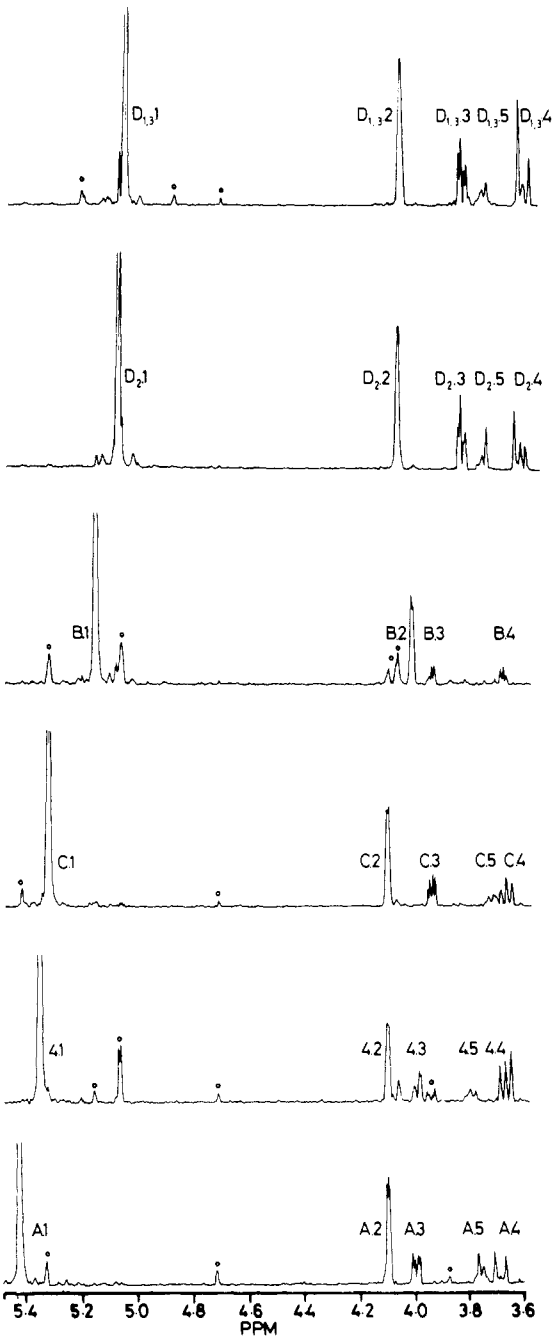

FIGURE 4: Cross sections along ω_1 from the RECSY spectrum of oligosaccharide VII. The correlation of H1 with H2, H3, H4, and H5 is illustrated for most residues. The additional assignments available from this method are used to assign cross-peaks in the NOESY and COSY spectra (Figure 3). The circled resonances arise from artifacts and cross-talk in the unsymmetrized spectrum.

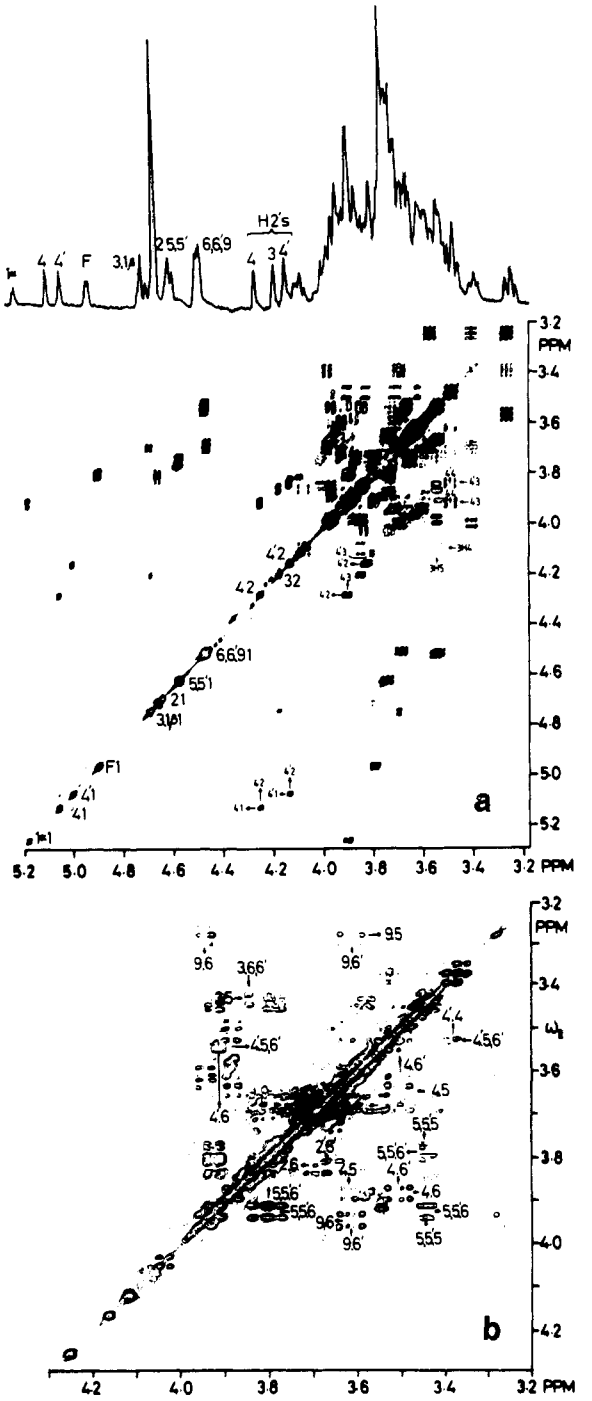

FIGURE 5: (a) COSY spectrum (region 3.2–5.2 ppm) of oligosaccharide VI. In contrast to the COSY spectra of unbisected structures, the majority of resonance assignments are available from this spectrum. In particular, the cross-peak correlating Man-3 H4 with Man-3 H5 ($\omega_1 \approx 3.55$ ppm, $\omega_2 = 4.07$ ppm) is well resolved, as shown. Nevertheless, the H6 protons cannot be unambiguously assigned. (b) TQCOSY spectrum (region 3.2–4.3 ppm) of oligosaccharide VI. The H6 protons of Man3 are now readily assigned, together with the H5 and H6 protons of the remaining residues, with the exception of GlcNAc-1. Assignments in the latter are complicated by an admixture of anomers.

values of J_{56} and J_{56}' could be obtained by one-dimensional spectral simulation.

An identical assignment procedure was used for II. It was again found that the H6 protons of Man-3 were magnetically equivalent. Also, the H3 and H4 protons formed a tightly coupled AB system. Thus, the multiplicity of the H5 proton (the X part of an approximate $ABXC_2$ system) was too complex and poorly resolved to allow the J values to be extracted, even by simulation. However, knowledge of the chemical shifts of H5 and the H6's for II allowed predictions to be made regarding the rotamer distributions, as discussed below.

The assignments and J's for the H5's and H6's of the six oligosaccharides are listed in Table I, together with the rotamer distributions about the α1–6 linkages, which are calculated from the J's by using the procedure described in the following section.

Rotamer Distributions. The observed values of J_{56} and J_{56}' for hydroxymethyl groups in monosaccharides and oligosaccharides are sensitive to the rotamer distributions about the C5–C6 bond. Predictions based upon empirical energy calculations (Marchessault & Perez, 1979) indicate that there

Table I: Chemical Shifts, J Values, and Rotamer Distributions for H5, H6, and H6′ Protons of Residues Shown[a]

structure	residue	chemical shift[b] (H5, H6, H6′)	J_{56}, $J_{56'}$[c]	rotamer distribution (%) 175°	−50°
I	Man-3	3.63			
		3.81	2.1, 5.8	40 ± 10	55 ± 20
		3.92			
II	Man-3	3.64			
		~3.90[d]	nd	~50	~50
		~3.90[d]			
III	Man-3	3.62			
		3.76	2.1, 5.8	40 ± 10	55 ± 20
		3.94			
	Man-4′	3.85			
		3.73	2.2, 5.8	45 ± 10	54 ± 20
		3.98			
IV	Man-3	3.64			
		3.82	2.1, 5.8	40 ± 10	55 ± 20
		3.96			
VI	Man-3	3.55			
		~3.90[d]	~2, ~2	100[e]	0
		~3.90[d]			
VII	Man-3	3.58			
		3.72	~2, ~2	100[e]	0
		4.02			
	Man-4′	~3.80[d]			
		3.71	~2, ~2	100[e]	0
		3.99			

[a] We should note that during the course of this study the resonance position of Man-4′ H5 (3.64 ppm) for the structure I was found to be inconsistent with that given (3.75 ppm) in our previous study. The cross-peak detected in the early study was generated by magnetization transfer through the tightly coupled Man-4′ H4–H5 spin system, followed by relayed transfer to H6. This discrepancy arises from the combined effects of an incomplete assignment strategy together with the poor stability of the 470-MHz spectrometer employed previously (Homans et al., 1984), which prevented the determination of the multiplicity of the cross-peaks in the 2D spectra. The self-consistent nature of the present assignments avoids such discrepancies. [b] Chemical shifts are given relative to acetone, δ = 2.225 ppm at 25 °C. [c] J values are measured to an accuracy of ±0.5 Hz (nd = not determined). The maximum and minimum limits of the J's were used to estimate the error in rotamer distributions. [d] Approximate values due to strong coupling. [e] It is difficult to estimate the error in these measurements since the J values approach the line widths.

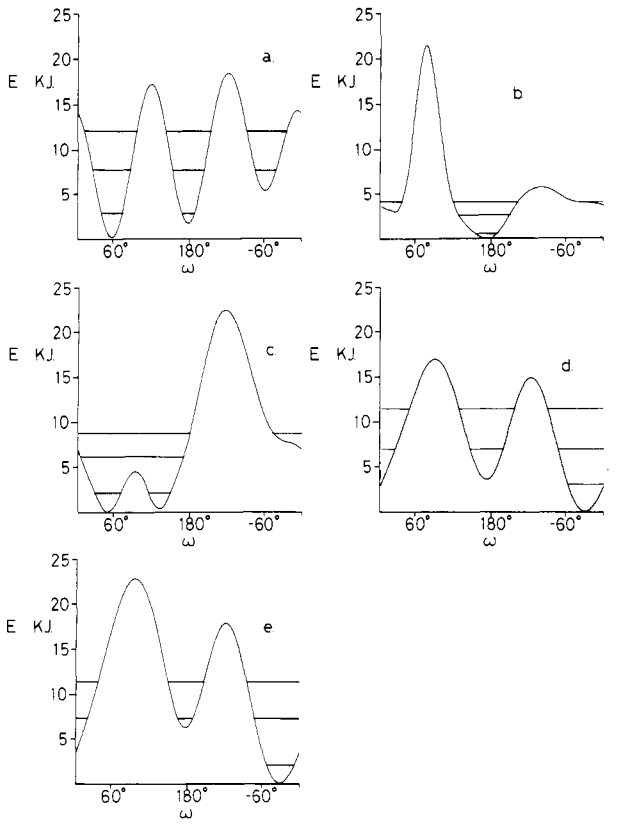

FIGURE 6: Potential energy profiles about the C5–C6 linkage in β-D-glucose calculated by using the following methods: (a) molecular mechanics (MM2) methods, with the dihedral angles H′4O4C4C5 = 180° and H′6O6C6C5 = 180°; (b) semiempirical quantum mechanical (MNDO) methods, for fixed optimized structure (see text), with the dihedral angles H′4O4C4C5 = 55° and H′6O6C6C5 = 60°; (c) As in (b), but with optimization of the bond lengths and angles of O4H′4 to assess the possibility of H bonding to the O6 with H′6O6C6C5 = 180°; (d) As in (b), but with the dihedral angle H′4O4C4C5 = 180° and H′6O6C6C5 = 180°, to exclude the formation of an intramolecular H bond from H′4 to O6; (e) As in (d) but calculated for the optimized geometry of β-D-mannose. In panels, the energy bounds for 70%, 95%, and 99% of the molecules are shown.

are three favorable torsional positions for the hydroxymethyl group in "gluco" monosaccharides, namely, ω = 180° (otherwise known as the gauche–gauche rotamer), ω = −60° (gauche–trans), and ω = 60° (trans–gauche). Using molecular mechanics (MM2) calculations, we have obtained similar results to those described in Marchessault and Perez (1979) for β-D-glucose (Figure 6a). It is notable that one of the predicted energy minima (trans–gauche) has not been found in a survey of over 100 crystal structures of "gluco" configuration carbohydrates (Marchessault & Perez, 1979). Marchessault and Perez (1979) have rationalized this anomaly by noting that the "Hassel–Ottar" effect, which is not explicitly included in the empirical calculations, will destabilize the trans–gauche rotamer by as much as 3 kcal/mol. However, these authors emphasize that the trans–gauche rotamer should not be systematically disregarded, due to the difficulty in estimating the magnitude of this effect. In contrast, Pincus et al. (1976) have suggested that the trans–gauche rotamer is stabilized by intraresidue hydrogen bonding. Since the inclusion or exclusion of the trans–gauche rotamer is crucial to the interpretation of our NMR data, we have used semiempirical quantum mechanical (MNDO) calculations to predict independently the conformational preferences of the hydroxymethyl group in β-D-glucose and β-D-mannose. We then use these predictions to interpret the J values shown in Table I for each oligosaccharide in terms of rotamer distributions.

Optimization of geometry (see Materials and Methods) for β-D-glucose using the crystal coordinates (Chu & Jeffrey, 1968) gave a global minimum with ω = 170° (Figure 6b) and the dihedral angles H′6O6C6C5 = 60° and H′4O4C4C5 = 55°. One other minimum was found at ω = 35° upon rotation of the hydroxymethyl group. However, with H′6O6C6C5 = 60°, formation of an α1–6 glycosidic linkage is sterically unfavorable, and this profile is therefore unlikely to be representative of structures containing an α1–6 linkage.

Further calculations showed that the overall energy profile was dependent upon the orientation of O6H′6 and O4H′4. Thus, in a second calculation, upon rotation of the hydroxymethyl group (with optimization of bond lengths and bond angles of O4H′4 and the dihedral angle H′6O6C6C5 = 180°) two further minima were found at ω = 45° and 135° (Figure 6c). These conformers are stabilized by the formation of a hydrogen bond between H′4 and O6. Finally, different minima were found when the orientation of O4H′4 was adjusted (H′4O4C4C5 = 180°) to minimize steric interactions and to exclude the formation of an intraresidue hydrogen bond. These minima occurred at ω = 170° and ω = −30° (Figure 6d).

Each of the conformers in Figure 6b–d will give rise to unique values of J_{56} and $J_{56'}$. We have calculated the angular dependence of these parameters using the modified Karplus

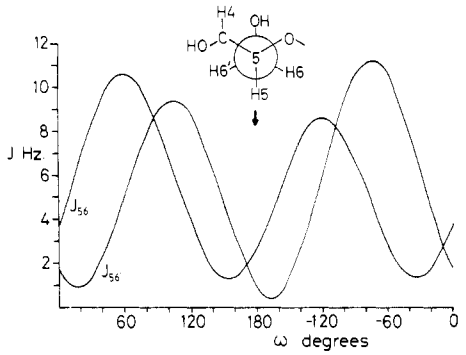

FIGURE 7: Angular dependence of J_{56} and $J_{56'}$ for "gluco" carbohydrates calculated by using the modified Karplus equation of Altona and Haasnoot (Altona & Haasnoot, 1980; Haasnoot et al., 1980). The stereochemistry is shown for $\omega = 180°$.

equation of Altona and Haasnoot (Altona & Haasnoot, 1980; Haasnoot et al., 1980) (Figure 7). The suitability of these functions is exemplified by the good agreement between the predicted values of J_{56} (10.7 Hz) and $J_{56'}$ (5.0 Hz) for $\omega = 60°$, compared with those obtained experimentally in a benzylidene derivative (Gagnaire et al., 1973), where $J_{56} = 11.0$ Hz and $J_{56'} = 5.0$ Hz for the same rotamer. Of the three predicted sets of rotamers, the first ($\omega = 170°$ and 35°) are sterically unfavorable in α1–6 linked structures since H'6O6C6C5 $\approx 60°$, and the second ($\omega = 135°$ and 45°) probably do not exist in aqueous solution, since these are both stabilized by intraresidue hydrogen bonding which will be in competition with solvent water. We therefore conclude that the third pair of rotamers ($\omega \approx 170°$ and $\omega \approx -30°$) are predominant in aqueous solution. These minima were essentially identical in β-D-mannose (Figure 6e). Notably, the profiles in Figure 6d,e accurately predict the instability of the $\omega = 60°$ rotamer in the absence of intramolecular hydrogen bonding, in contrast to the empirical MM2 method (Figure 6a).

By use of the functions shown in Figure 7, the experimentally determined J values were used to determine the relative distributions of rotamers by iteratively fitting these J's to the closest values of ω consistent with the above predictions by using a small microprogram. This calculation was performed twice for each of the possible values of J_{56} and $J_{56'}$ (due to the ambiguity in assignment of the H6's). Only one pair of J values was found to fit with rotamer distributions close to the predicted minima. These are shown for each oligosaccharide in Table I, together with the defined resonance assignments for the H6 protons. Notably, in several of the structures studied (I, III, IV, and VII) the relative H6 proton resonance assignments for Man-3 are essentially reversed in comparison with β-D-mannose. A similar conclusion was reached by Winnik et al. (1982) in the synthetic methyl trimannoside (Manα1–6)Manα1–3Manα1–O-Me, although assignment details were not given. Conversely, the resonance assignments obtained by Bock et al. (1982) in similar compounds are at variance with those proposed in the present study.

Since the values of J_{56} and $J_{56'}$ could not be determined in II, the rotamer distributions about C5–C6 of Man-3 in this compound could not be measured directly. However, the differences in rotamer populations for the α1–6 linkage between the oligosaccharides considered here generate characteristic chemical shift differences, and we have used these to determine the rotamer distributions in II. In VI, where ω is restricted to 175°, the H3 and H4 protons of Man-3 resonate at 3.88 and 4.07 ppm, respectively. In contrast, these protons resonate at 3.77 and 3.88 ppm, respectively, in VII, where ω is also restricted to 175°. In I, III, and V, where ω averages between 175° and −50°, the H3 and H4 protons form a strongly coupled AB system at ~3.77 ppm. As noted previously (Brisson & Carver, 1983b), the downfield shift of Man-3 H4 in structures with $\omega = 175°$ can be interpreted in terms of the proximity of the hydroxymethyl oxygen to this proton. In VI, both the H3 and H4 protons of Man-3 are additionally shifted by the proximity of the "bisecting" GlcNAc. Thus, the resonance positions of Man-3 H3 and H4 in II, which form an AB system at ~3.88 ppm, are downfield-shifted (in comparison with I, III, and V) by the presence of the bisecting GlcNAc, but no *additional* downfield shift is experienced by Man-3 H4. It is concluded that the value of ω is not restricted to 175° in II but averages between 175° and −50°.

Finally, we should note that the rotamer distributions in all of these oligosaccharides may differ in aprotic solvents, due to the possibility of hydrogen-bond stabilization of alternative rotamers (see above).

Discussion

In summary, we have described a proton resonance assignment strategy for each of the three classes of oligosaccharide under investigation. These assignments have allowed for the determination of the mutual spin–spin couplings between the H5 and H6 protons at all of the α1–6 linkages for each compound. These parameters, together with the results of semiempirical quantum mechanical (MNDO) energy calculations in model monosaccharides, have been used to calculate the rotamer distributions at each α1–6 linkage.

The results of the conformational analyses are summarized diagrammatically in Figure 8. Each numbered structure corresponds with that shown in Figure 1. Averaging between rotamer pairs is illustrated by dotted lines and double-headed arrows. Thus, in the case of III, averaging about both α1–6 linkages occurs. This result contrasts with that proposed for III when in a *glycopeptide*, where it was concluded (Brisson & Carver, 1983b) that, for the Manα1–6Manβ– linkage, ω is restricted to −60° (i.e., a fixed conformation). Chemical shift data suggest however that the latter conclusion is erroneous. In VII, where $\omega = 175°$, Man-3 H4 resonates at 3.88 ppm due to deshielding by the hydroxymethyl oxygen. In IV, where $\omega = 175°$ and −50°, Man-3 H4 resonates with a fast-exchange *average* shift of 3.77 ppm. Thus, if ω was restricted to −60° in III, then Man-3 H4 would be required to resonate at around 3.66 ppm. However, the measured chemical shift of Man-3 H4 for III in both the present study and that described previously (Brisson & Carver, 1983b) is 3.77 ppm, which is entirely consistent with the motional averaging suggested by the J values in Table I. By a similar argument, it is highly probable that the bisected hybrid structure examined previously (Brisson & Carver, 1983b) (a glycopeptide of structure VIII) also exists with $\omega = 175°$ and −50°, since in this case the reported chemical shifts for Man-3 H3 and H4 in VIII are identical with those in II. We have therefore included structure VIII in Figure 8. In addition, the data obtained by Brisson and Carver (1983b) for V are identical with those obtained for IV in the present study, and V is therefore also included for completeness in Figure 8.

On examination of Figure 8, it is apparent that the overall conformations of the oligosaccharides studied are dependent upon certain "key" residues in the primary sequence. Conversely, other residues do not appear to alter the secondary structure dramatically. Primary sequence changes of this latter class might thus be termed "type 1" structural changes and

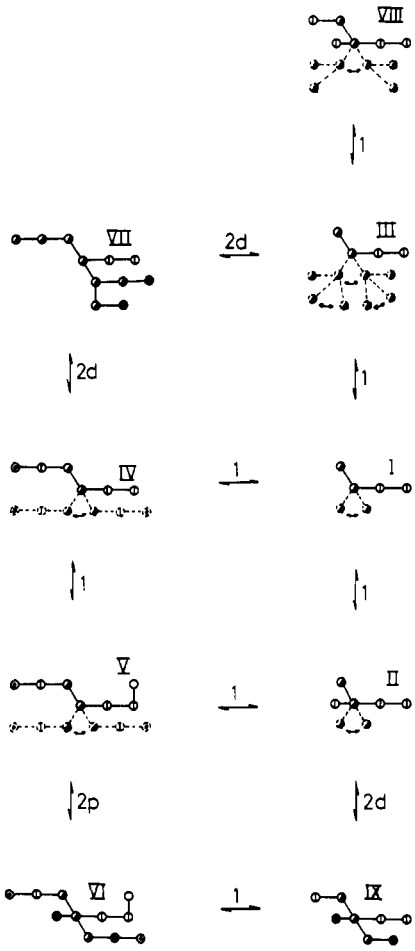

FIGURE 8: Conformational transitions between oligosaccharides considered in the present study. The number of each structure corresponds with that shown in Figure 1. Types 1, 2p, and 2d structural changes are shown in the figure. Averaging of the α1–6 linkages between two conformations is represented by dotted lines and double-headed arrows. Thus, in structure III, averaging occurs about both α1–6 linkages. Although this may also be the case in structure VIII, no experimental evidence is available to suggest that averaging occurs about the Manα1–6Manα linkage, and this is therefore not illustrated. In the cases of type 2 changes, the black circles represent residues that are responsible for the conformational transitions, i.e., two Manα1–2– residues in structure VII and GlcNAcβ1–4–(bisecting GlcNAc) and GlcNAcβ1–2 residues in structures VI and IX. The key to the remaining residues is as follows: ●, mannose; ⊙, galactose; ◆, *N*-acetylglucosamine; ○, fucose.

are labeled as such in Figure 8. However, those primary sequence changes that alter the *overall* solution conformation might be termed "type 2" changes, and these are of two types. For example, the addition of a bisecting GlcNAc to structure V, thus generating VI, is termed a "type 2p" change, since the site of conformational variance (the α1–6 linkage) is proximal to the site of glycosylation. Conversely, the addition of two Manα1–2 residues to structure III, thus generating structure VII, is termed a "type 2d" change, since the additional sites of glycosylation are distal to a conformational change at the Manα1–6Manβ– linkage. This profound and unexpected result bears a resemblance to an allosteric transition in proteins.

It is notable that the overall effect on the secondary structure of the addition or deletion of a given residue is not necessarily constant but depends upon the "starting structure". Thus, addition of a bisecting GlcNAc to I, thereby generating II, is a type 1 change, whereas this equivalent operation on V (generating VI) is a type 2p change. The latter change can only be explained in terms of cooperativity of the bisecting GlcNAc and either the Gal or GlcNAc residue of the α1–6 arm in VI. In this regard, the "bisected" structure examined by Strecker et al. (1977) (which is structure IX of Figure 8 minus GlcNAc-1) shows a downfield-shifted resonance at ~4.07 ppm, corresponding to the resonance position of Man-3 H4. As in VI, this shift is accounted for by the restriction of ω to 175°. It can therefore be concluded that *both* a bisecting GlcNAc *and* an α1–6 arm GlcNAc are required in biantennary bisected structures to create a type 2p change. In contrast, the addition of Manα1–2 residues to the terminal mannose residues of the Manα1–6Manβ– arm of III is sufficient to restrict *both* α1–6 linkages in VII to ω = 175°.

The mechanisms that result in any of these type 2 changes have not been fully elucidated. However, arm–core interactions may be an important feature. These have been implied in structure VII (minus GlcNAc-1) from careful 1D NMR studies and have been termed "anomerization effects" by Vliegenthart et al. (1983). In the present study, we have also noted large chemical shift perturbations upon GlcNAc-5′ in the α1–6 arm in VI. Whereas the H3 protons of GlcNAc-5 and GlcNAc-5′ both resonate at 3.76 ppm in IV, the H3 proton of GlcNAc-5′ is upfield-shifted to 3.66 ppm in VI. This may be indicative of an interaction between GlcNAc-5′ and GlcNAc-2 of the core. In addition to these observations, model building studies (Homans et al., unpublished observations) suggest that steric factors might also be important in determining the absolute configuration for type 2 (particularly 2p) changes.

In the absence of experimental data from suitable model systems for oligosaccharide–receptor interactions, the biological relevance of the above in terms of these interactions is difficult to assess at present. However, the types of structural change shown in Figure 8 may confer tolerance of these systems to the phenomenon of microheterogeneity. It is well-known that a manifold of structures usually exists at a single glycosylation site on a protein. If each primary structure were to generate an unique solution conformation, an extraordinarily large variety of recognition phenomena would be presumed to exist at a given glycosylation site. However, *overall* conformational changes (types 2p and 2d), generated by a few key residues in the primary sequence, would restrict the diversity in secondary structure to a more limited subset. In this regard it must be noted that although few lectin specificities have been well characterized to date, several related structures are generally found to act as ligands.

Finally, we find that there is no correlation between the four classes of primary monosaccharide structure discussed here (i.e., complex, bisected complex, high mannose, and hybrid) and their respective secondary structures. Indeed, the major conformational changes occur within classes. In probing the relationship between oligosaccharide structure and the proposed recognition function in biological systems, it is clear that seemingly small changes in primary sequence may be highly significant in terms of the three-dimensional structure.

APPENDIX

Triple Quantum Filtered COSY. Multiple quantum filtered COSY, as described in Piantini et al. (1982), can be achieved with the pulse sequence $90°_{\theta}$–t_1–$90°_{\theta+\zeta}$–Δ–$90°_{\zeta}$–t_2(acquisition). For a triple quantum filter, θ is cycled in steps of $\pi/3$ radians. The resulting free induction decays are alternately added and subtracted. In order to achieve quadrature detection in t_1, the cycle is repeated with $\zeta = \pi/2$ rad, and the receiver reference phase is cycled in the normal manner in order to selectively detect the coherence transfer echo (Maudsley et al., 1978).

Although the nonexchangeable protons within a given hexose represent a seven-spin system, the essential aspects of the triple

quantum filter can be understood with reference to a loosely coupled three-spin system, *ISM*. The first pulse creates single quantum (transverse) magnetization which evolves under $H = H_Z + H_J$ during the t_1 period (where H_z and H_J are the usual Zeeman and spin coupling Hamiltonians). In the absence of a refocusing pulse, the second pulse creates all orders of multiple quantum coherence.

With respect to the creation of triple quantum coherence, the relevant terms of the reduced density operator just after the second pulse may be described explicitly by operator products (Sørensen et al., 1983):

$$\sigma_1 = -4I_xM_yS_y \sin \pi J_{IS}t_1 \sin \pi J_{IM}t_1 \sin \omega_I t_1 - 4S_xM_yI_y \sin \pi J_{IS}t_1 \sin \pi J_{SM}t_1 \sin \omega_S t_1 - 4M_xI_yS_y \sin \pi J_{SM}t_1 \sin \pi J_{IM}t_1 \sin \omega_M t_1 + \text{other terms} \quad (1)$$

where the ω's refer to the Larmor precession frequencies of the respective spins. Each of the three terms in eq 1 consists of a superposition of pure triple quantum coherence and single quantum combination lines. This can be demonstrated in terms of raising and lowering operators. For example, the first term of eq 1 can be expanded thus:

$$-4I_xM_yS_y = \tfrac{1}{2}(I^+I^+I^+ + I^-I^-I^- - I^+I^+I^- - I^+I^-I^+ + I^+I^-I^- + I^-I^+I^+ - I^-I^+I^- - I^-I^-I^+) \quad (2)$$

During the course of the phase cycle ϕ, all terms are canceled except those corresponding to a state of pure triple quantum coherence:

$$3QT_x = \tfrac{1}{2}(I^+I^+I^+ + I^-I^-I^-) \sin \pi J_{IS}t_1 \sin \pi J_{IM}t_1 \sin \omega_I t_1 = \tfrac{1}{4}(4I_xS_xM_x - 4I_xS_yM_y - 4I_yS_xM_y - 4I_yS_yM_x) \sin \pi J_{IS}t_1 \sin \pi J_{IM}t_1 \sin \omega_I t_1 \quad (3)$$

The last three terms on the right-hand side of eq 3 are converted into observable antiphase transverse magnetization by the final pulse:

$$\sigma_2 = (-4I_xS_zM_z - 4I_zS_xM_z - 4I_zS_zM_x) \sin \pi J_{IS}t_1 \sin \pi J_{IM}t_1 \sin \omega_I t_1 \quad (4)$$

Similar expressions exist for the magnetization components that arise from S_z and M_z (second and third terms in eq 1). The three terms in eq 4 evolve during the detection period with Larmor precession frequencies ω_I, ω_S, and ω_M, respectively. The first term thus corresponds to a diagonal peak after two-dimensional Fourier transformation, and the second and third terms correspond to cross-peaks. The latter are seen to contain antiphase magnetization with respect to J_{IS}, J_{SM}, and J_{IM} and cannot therefore give rise to detectable magnetization unless these couplings are resolved. This leads directly to the selection rules described by Piantini et al. (1982). In terms of the COSY spectra of oligosaccharides, this result shows that cross-peaks can only arise in three quantum filtered spectra from protons 5, 6, and 6′, since these are generally the only protons that have mutual, resolved couplings.

Registry No. I, 70858-45-6; II, 102038-83-5; III, 66091-47-2; IV, 71496-53-2; VI, 76149-64-9; VII, 71246-55-4.

References

Allinger, N. L., & Yuh, Y. H. (1981) *QCPE 13*, 395.

Altona, C., & Haasnoot, C. A. G. (1980) *Org. Magn. Reson. 13*, 417.

Bax, A., & Freeman, R. (1981) *J. Magn. Reson. 44*, 542.

Bock, K., Arnarp, J., & Lonngren, J. (1982) *Eur. J. Biochem. 129*, 171.

Brisson, J.-R., & Carver, J. P. (1983a) *Biochemistry 22*, 3671.

Brisson, J.-R., & Carver, J. P. (1983b) *Biochemistry 22*, 3680.

Chu, C., & Jeffrey, G. A. (1968) *Acta Crystallogr., Sect. B: Struct. Crystallogr. Cryst. Chem. B24*, 830.

Dewar, M. J. S., & Thiel, W. (1977) *J. Am. Chem. Soc. 99*, 4899.

Dewar, M. J. S., Zoebisch, E. G., Healy, E. F., & Stewart, J. J. P. (1985) *J. Am. Chem. Soc. 107*, 3902.

Dorland, L., van Halbeek, H., Vliegenthart, J. F. G., Lis, H., & Sharon, N. (1981) *J. Biol. Chem. 256*, 7708.

Feizi, T. (1981) *Trends Biochem. Sci. (Pers. Ed.) 6*, 333.

Fukuda, M., & Fukuda, M. N. (1984) in *The Biology of Glycoproteins* (Ivatt, R. J. Ed.) pp 183–224, Plenum Press, New York and London.

Gagnaire, D., Horton, D., & Taravel, F. R. (1973) *Carbohydr. Res. 27*, 363.

Haasnoot, C. A. G., De Leeuw, F. A. A. M., & Altona, C. (1980) *Tetrahedron 36*, 2783.

Homans, S. W., Dwek, R. A., Fernandes, D. L., & Rademacher, T. W. (1982) *FEBS Lett. 150*, 503.

Homans, S. W., Dwek, R. A., Fernandes, D. L., & Rademacher, T. W. (1983a) *FEBS Lett. 164*, 231.

Homans, S. W., Dwek, R. A., Fernandes, D. L., & Rademacher, T. W. (1983b) *Biochim. Biophys. Acta 760*, 256.

Homans, S. W., Dwek, R. A., Fernandes, D. L., & Rademacher, T. W. (1984) *Proc. Natl. Acad. Sci. U.S.A. 81*, 6286.

Ivatt, R. J. (1984) in *The Biology of Glycoproteins* (Ivatt, R. J., Ed.) pp 95–161, Plenum Press, New York and London.

Liang, C.-J., Yamashita, K., & Kobata, A. (1980) *J. Biochem. (Tokyo) 88*, 51.

Marchessault, R. H., & Perez, S. (1979) *Biopolymers 18*, 2369.

Maudsley, A. A., Wokaun, A., & Ernst, R. R. (1978) *Chem. Phys. Lett. 55*, 9.

Müller, L., & Ernst, R. R. (1980) *Mol. Phys. 38*, 963.

Paulsen, H., Peters, T., Sunwell, V., Lebuhn, R., & Meyer, B. (1984) *Liebigs. Ann. Chem. 5*, 951.

Piantini, U., Sørensen, O. W., & Ernst, R. R. (1982) *J. Am. Chem. Soc. 104*, 6800.

Pincus, M. R., Burgess, A. W., & Scheraga, H. A. (1976) *Biopolymers 15*, 2485.

Richards, W. G., & Ganellin, C. R. (1974) in *Molecular and Quantum Pharmacology* (Bergman, E. D., & Pullman, B., Eds.) pp 391–400, Reidel, Dordrecht, Holland.

Sørensen, O. W., Eich, G. W., Levitt, M. H., Bodenhausen, G., & Ernst, R. R. (1983) *Prog. Nucl. Magn. Reson. Spectrosc. 16*, 163.

States, D. J., Haberkorn, R. A., & Ruben, D. J. (1982) *J. Magn. Reson. 48*, 286.

Stewart, J. J. P. (1984) *QCPE Bull.*, 455.

Strecker, G., Herlant-Peers, M.-C., Fournet, B., Montreuil, J., Dorland, L., Haverkamp, J., Vliegenthart, J. F. G., & Farriaux, J. P. (1977) *Eur. J. Biochem. 81*, 165.

Szulman, A. (1980) *Current Top. Dev. Biol. 14*, 127.

Vliegenthart, J. F. G., Dorland, L., & van Halbeek, H. (1983) *Adv. Carbohydr. Chem. Biochem. 41*, 209.

Winnik, F. M., Brisson, J.-R., Carver, J. P., & Krepinsky, J. J. (1982) *Carbohydr. Res. 103*, 15.